



HHS Public Access

Author manuscript

Mitochondrial Commun. Author manuscript; available in PMC 2024 March 18.

Published in final edited form as:

Mitochondrial Commun. 2024 ; 2: 1–13. doi:10.1016/j.mitoco.2024.01.001.

Structural determinants of mitochondrial STAT3 targeting and function

Isabelle J. Marié^a, Tanaya Lahiri^a, Özlem Önder^b, Kojo S.J. Elenitoba-Johnson^b, David E. Levy^{a,*}

^aDepartment of Pathology and Perlmutter Cancer Center, NYU Grossman School of Medicine, New York, NY, 10128, USA

^bDepartment of Pathology and Laboratory Medicine, Perelman School of Medicine at the University of Pennsylvania, Philadelphia, PA, 19104, USA

Abstract

Signal transducer and activator of transcription (STAT) 3 has been found within mitochondria in addition to its canonical role of shuttling between cytoplasm and nucleus during cytokine signaling. Mitochondrial STAT3 has been implicated in modulation of cellular metabolism, largely through effects on the respiratory electron transport chain. However, the structural requirements underlying mitochondrial targeting and function have remained unclear. Here, we show that mitochondrial STAT3 partitions between mitochondrial compartments defined by differential detergent solubility, suggesting that mitochondrial STAT3 is membrane associated. The majority of STAT3 was found in an SDS soluble fraction copurifying with respiratory chain proteins, including numerous components of the complex I NADH dehydrogenase, while a minor

This is an open access article under the CC BY-NC-ND license (<http://creativecommons.org/licenses/by-nc-nd/4.0/>).

*Corresponding author. Department of Pathology, NYU Grossman School of Medicine, 550 1st Ave MSB-553A, New York, NY, 10016, USA. david.levy@nyulangone.org (D.E. Levy).

Consent to participate

None of the experiments described in this study required consent to participate.

Ethics approval

All experiments with animals involved protocols approved by the NYU Langone Health Institutional Animal Care and Use Committee and were designed in accordance with recommendations from AAALAC International and the Public Health Service animal welfare guidelines. All experiments with recombinant DNA were conducted under approval by the Institutional Biosafety Committee of NYU Langone Health.

CRedit authorship contribution statement

Isabelle J. Marié: Conceptualization, Data curation, Formal analysis, Investigation, Methodology, Supervision, Validation, Writing – original draft, Writing – review & editing. **Tanaya Lahiri:** Data curation, Formal analysis, Investigation, Methodology, Validation, Writing – original draft, Writing – review & editing. **Özlem Önder:** Data curation, Investigation, Methodology, Visualization, Writing – review & editing. **Kojo S.J. Elenitoba-Johnson:** Conceptualization, Data curation, Funding acquisition, Methodology, Project administration, Supervision. **David E. Levy:** Conceptualization, Data curation, Formal analysis, Funding acquisition, Investigation, Methodology, Project administration, Resources, Supervision, Validation, Writing – original draft, Writing – review & editing.

Declaration of generative AI and AI-assisted technologies in the writing process

During the preparation of this work the author(s) used Writefull[®] by Writefull BV in order to spell-check the manuscript. After using this tool/service, the author(s) reviewed and edited the content as needed and take(s) full responsibility for the content of the publication.

Declaration of competing interest

The authors declare no conflicts of interest.

Appendix A. Supplementary data

Supplementary data to this article can be found online at <https://doi.org/10.1016/j.mitoco.2024.01.001>.

component was found with proteins of the mitochondrial translation machinery. Mitochondrial targeting of STAT3 required the amino-terminal domain, and an internal linker domain motif also directed mitochondrial translocation. However, neither the phosphorylation of serine 727 nor the presence of mitochondrial DNA was required for the mitochondrial localization of STAT3. Two cysteine residues in the STAT3 SH2 domain, which have been previously suggested to be targets for protein palmitoylation, were also not required for mitochondrial translocation, but were required for its function as an enhancer of complex I activity. These structural determinants of STAT3 mitochondrial targeting and function provide potential therapeutic targets for disrupting the activity of mitochondrial STAT3 in diseases such as cancer.

Keywords

Mitochondrial import; Stat3; Electron transport chain

1. Introduction

Signal transducer and activator of transcription (STAT)¹⁻³ is a transcription factor that has been implicated in a number of cellular processes such as inflammation and tumorigenesis. STAT3 exists as two major isoforms translated from a single gene¹⁻³ a full-length 770 amino acid protein (STAT3 α) and a carboxyl-terminally truncated protein of 722 amino acids (STAT3 β) that substitutes a unique 7 amino acid sequence for the 48 terminal amino acids of the full-length isoform.⁴ Canonical functions of STAT3 largely occur in the cytoplasm and nucleus, with STAT3 being activated by protein tyrosine phosphorylation in response to stimulation of cytokine receptors, mediated largely by JAK protein tyrosine kinases.⁵ Tyrosine phosphorylation of residue 705 stimulates the formation of an active dimer through interaction with the SH2 domain of a sister molecule and the resulting dimerization triggers translocation and retention of STAT3 in the nucleus.⁶ Nuclear dimeric STAT3 recognizes a palindromic consensus DNA sequence known as a gamma-activated site or GAS,⁷ which is commonly located upstream of promoter regions of STAT3-stimulated genes. Many STAT3-stimulated genes are involved in inflammatory responses, growth control, and malignancy.⁸ Some genes can also be regulated by STAT3 in the absence of tyrosine phosphorylation.^{9,10} In addition to tyrosine phosphorylation, STAT3 is serine phosphorylated on S727, a modification that enhances a number of STAT3 functions.

In addition to its nuclear functions, non-transcriptional roles of STAT3 α have been highlighted by its presence in multiple organelles such as lysosomes,¹¹ endoplasmic reticulum (ER),¹² mitochondria-associated membranes (MAM)¹³ and mitochondria.¹⁴⁻¹⁶ Although the functional consequences of its role(s) in organelles remain somewhat controversial,^{17,18} there is ample evidence that STAT3 plays a metabolic role from within mitochondria. Indeed, STAT3 has been shown to modulate the activity of complexes I, II and V of the electron transport chain and to regulate cellular redox homeostasis.^{15,16,19-21} Mitochondrial STAT3 contributes to cellular transformation and cardiomyocyte protection, among other physiological processes.^{15,16,22-25} Interestingly, although tyrosine phosphorylation is dispensable for STAT3 mitochondrial functions, serine 727 phosphorylation appears to be essential for most functions.^{22,26,27} Both the nuclear

and the mitochondrial functions of STAT3 contribute to malignant transformation, cancer cell growth and survival, and metastasis.²⁸ As such, STAT3 is recognized as a viable chemotherapeutic target.²⁹

Most mitochondrial proteins, including STAT3, are encoded by the nuclear genome and are subsequently imported into mitochondria following translation in the cell cytoplasm. Most proteins targeted to the mitochondria depend on N-terminal extensions of 10–40 amino acids referred as mitochondrial targeting sequences (MTS) or pre-sequences. These pre-sequences are typically rich in positively charged amino acid residues forming amphipathic α -helices important for their interaction with the mitochondrial translocation machinery. Proteins initially enter mitochondria using the translocase of the outer membrane (TOM) complex which includes the pore-forming protein Tom40.³⁰⁻³² Once in the inter-membrane space, some proteins that are destined for matrix or inner membrane localization can be transferred to the translocase of the inner membrane composed of the TIM23 complex.³³⁻³⁷ Following passage through or into the inner mitochondrial membrane, cleavage of the pre-sequence by a matrix peptidase typically occurs.³⁸ However, a significant number (around 30–40 %) of proteins homing to mitochondria do not contain an amino-terminal pre-sequence but rather rely on one or multiple poorly defined internal motifs to translocate into mitochondria via a mechanism that is not yet completely understood. STAT3 belongs to this second class of mitochondrial proteins and, so far, the exact process by which it translocates to mitochondria still eludes us. STAT3 has been shown to interact with Tom20 and gene associated with retinoid-interferon induced mortality (Grim) 19, an accessory protein associated with respiratory complex I,^{39,40} suggesting that both proteins could play roles in STAT3 import into mitochondria. However, it is commonly accepted that Tom20 is implicated in the translocation of proteins containing a N-terminal pre-sequence, whereas Tom70 mediates the import of proteins containing internal mitochondrial targeting motifs. Mapping the structural requirements for STAT3 mitochondrial import would provide important insights into the mechanism of translocation. Moreover, this information could potentially allow design of STAT3 isoforms with restricted localization to either cytoplasm and nucleus versus mitochondria, which could be an invaluable tool to discriminate between its metabolic and transcriptional functions in physiology and cancer.

In this study, we report that mitochondrial STAT3 likely exists as a homodimer or multimeric complex that partitions between an NP40 soluble fraction and an NP40 insoluble but SDS soluble protein fraction. We show that two distinct domains appear important for mitochondrial localization: the N-terminal domain and the linker domain. Last, whereas S727 phosphorylation has been shown to be essential for mitochondrial STAT3 functions, its absence does not affect STAT3 abundance in mitochondria.

2. Material and methods

2.1. Materials

All chemicals were purchased from Sigma-Aldrich (St. Louis, MO, USA) unless otherwise specified. Reagents with limited water solubility were initially dissolved in dimethylsulfoxide or ethanol before dilution in cell growth media (final solvent concentrations <0.1 %).

2.2. Cell culture

Cells were cultured in Dulbecco's Modified Eagle Medium (DMEM; GE Healthcare, Piscataway, NJ, USA) supplemented with 10 % Bovine Calf Serum (Sigma-Aldrich) and Gentamicin (Cellgro, Corning Life Sciences, Tewksbury, MA, USA) in a 95 % air/5 % CO₂ humidified atmosphere. The human triple-negative breast cancer cell line MDA-MB-231, human osteosarcoma cell line 143b, and human embryonic kidney cell line HEK293T were obtained from the American Type Culture Collection (Manassas, VA, USA). STAT3-null (KO) MDA-MB-231 and HEK293 cells were produced by CRISPR/cas9 mutagenesis by using guide RNA against *STAT3* (gRNA sequence: AGATTGCCCGGATTGTGGCC) and selection with 5 µg mL⁻¹ of puromycin.²⁰ MDA-MB-231 KO cells stably re-expressing STAT3²⁰ were maintained in media supplemented with 200 µg mL⁻¹ of hygromycin. Where indicated, cells were treated with 50 nM Calyculin A for 30 min. Rho0 cells lacking mitochondrial DNA (ρ0) were generated by culturing MDA-MB-231 cells in the presence of 50 µM dideoxycytidine (Sigma-Aldrich) and 1 mM uridine (Thermo-Fisher), as described.⁴¹ After 10 d, a cell sample was assayed for the absence of mitochondrial DNA by qPCR using primers for the hypervariable region of the replication origin (HVRF AATGTCTGCACAG CCACTTTCCAC, HVRR TCGTAGTGTCTGGCGAGCAGTTT) normalized to the nuclear gene beta-2-microglobulin (B2M) (Forward TGCTGTCT CCATGTTTGATGTATCT, Reverse TCTCTGCTCCCCACCTCTAAGT).

2.3. Animals

Wild type C57BL6/J mice and STAT3-S727A knock-in mice on a C57BL6/J background were bred in house under specific pathogen free conditions at NYU Langone Health. Individual mice were euthanized by CO₂ inhalation followed by cervical dislocation prior to tissue harvest. All animal protocols followed guidelines from AAALAC International and the Public Health Service and were approved in advance by the NYU Langone Health Institutional Animal Care and Use Committee.

2.4. Mitochondrial preparation

Cells were harvested and washed once with PBS. The cell pellet was resuspended in mitochondria purification buffer (MPB: 10 mM Tris, 1 mM EGTA, 200 mM sucrose, pH 7.4) containing freshly added protease inhibitors (Thermo Fisher), 2 mM Na₃VO₄, 1 mM DTT, and 1 mM sodium-β-glycerophosphate, and incubated on ice for 10 min. The cell suspension was disrupted with 40 strokes in a Dounce homogenizer and centrifuged at 800 *g* for 5 min to pellet nuclei and unbroken cells. The supernatant was transferred to a fresh tube and spun at 10 000 *g* for 10 min to pellet mitochondria. Mitochondria were resuspended in MPB with 0.02 % digitonin and incubated on ice for 5 min, and spun at 10 000 *g* for 10 min. Mitochondria were washed 2 × with MPB to remove any digitonin, and protein content was quantified by using the Bio-Rad Coomassie dye assay.

2.5. Mitochondrial extraction

For differential lysis of mitochondria, purified mitochondria were thawed on ice, and resuspended in 1x volume of IBC buffer (10 mM Tris-MOPS, 1 mM EGTA/Tris, 200 mM sucrose, pH 7.4). Mitochondria suspensions were lysed in 1 % NP-40 lysis buffer by

incubating on ice for 15 min. After lysis, the supernatant was centrifuged at 15000 rpm for 15 min, and the clear supernatant was recovered. The pellet was resuspended in 1 % SDS containing RIPA-lysis buffer (50 mM Tris-HCl, 150 mM NaCl, 0.2 % SDS, 0.5 % sodium deoxycholate, 1 % Triton X-100, 5 % glycerol) by incubating on ice for 15 min. After lysis, the supernatant was centrifuged at 15000 rpm for 15 min, and the clear supernatant recovered. The remaining pellet was resuspended in 2x volume of Laemmli buffer prior to analysis by SDS-PAGE. Where indicated, mitochondria were further purified prior to lysis by treatment with digitonin and trypsin, or by treatment with digitonin and trypsin followed by sucrose gradient purification, as previously described.^{42,43}

2.6. Western blot analysis and antibodies

For western blot analysis, mitochondria or cell pellets were lysed in RIPA buffer containing freshly added protease inhibitors (Thermo Fisher), 2 mM Na₃VO₄, 1 mM DTT and 1 mM sodium-β-glycer-ophosphate, and incubated on ice for 10 min. Lysates were spun at 20 000 *g* for 10 min, and clarified lysates were resolved on SDS/PAGE, transferred to polyvinylidene fluoride membranes, blocked with 5 % milk, and probed with the antibodies. Unless otherwise specified, all antibodies and detection reagents were used at 1:2000 dilution prepared in 5 % BSA in TBST: STAT3-α (D1A5) (CST, Danvers, MA, USA, catalog no. 8768S), STAT3 (124H6) (CST, catalog no. 9139S), pS727-STAT3 (CST, catalog no. 9134) NDUFV2 (ABclonal, Woburn, MA, USA, catalog no. A7442), NDUFS2 (ABclonal, catalog no. A12858), SDHA (ABclonal, catalog no. A2594), Tubulin (Sigma, catalog no. 26628228), ERK1 (ABclonal catalog no. A0228), ATP5A1 (ABclonal catalog no. A5884), COXVa (ABclonal catalog no. A6437), ATP5B (ABclonal catalog no. A5769), PDE (ABclonal catalog no. A20888), Cytc1 (ABclonal catalog no. A10449), TFAM (ABclonal catalog no. A1926), Tom20 (ABclonal catalog no. A18047), Flag (Sigma-Aldrich catalog no. F1804), UBQCR2 (ABclonal catalog no. A4181), COX4I1 (ABclonal catalog no. A6564), CalR (ABclonal catalog no. 1066). The blots were developed using a chemiluminescent detection kit (Advansta WesternBright ECL HRP substrate) on a LI-COR Odyssey[®] Fc Imaging System.

2.7. Bio ID constructs

MTS.STAT3.Bio was constructed by fusing the sequence for MTS-STAT3-Flag¹⁵ to BioID2⁴⁴ in a lentiviral vector carrying puromycin resistance. MTS.TruncSTAT3.Bio was constructed by fusing the sequence for MTS-STAT3 truncated at amino acid 531 to Flag-BioID2 in a lentiviral vector carrying puromycin resistance. MDA-MB-231 STAT3 WT cells were infected to stably express the BioID fusion proteins and were maintained under 5 μg mL⁻¹ of puromycin.

2.8. Gene expression analysis

For quantitative reverse transcriptase-polymerase chain reaction (RT-PCR) analyses, total RNA was isolated using TriZol (Thermo Fisher) and reverse-transcribed with Moloney murine leukemia virus (M-MLV). The resulting cDNAs were amplified by qRT-PCR with SYBR green (Molecular Probes, Eugene, OR, USA) using the following primers: SOCS3 Forward CCACTCTTCAGCATCTCTGT, Reverse AGCTGGGTGACTTTCTCATA and beta-2-microglobulin (B2M) Forward TGCTGT CTCCATGTTTGATGTATCT, Reverse

TCTCTGCTCCCCACCTCTAAGT. Relative expression was determined by comparison to a standard curve generated from serial dilutions of cDNA containing abundant target sequences and normalized to the expression of B2M.

2.9. In vitro import assay

Full length STAT3, GFP and Slc, as well as different fragments of STAT3 fused to GFP, were cloned under the T7 promoter. *In vitro* translation was carried out in presence of ³⁵S-methionine in rabbit reticulocyte lysates for 90 min at 30 °C. Labeled proteins were incubated with 50 µg of mitochondria in import buffer (3 % BSA (fatty acid free), 250 mM sucrose, 80 mM KCl, 5 mM MgCl₂, 2 mM KH₂PO₄, 5 mM methionine, 10 mM MOPS-KOH pH 7.2, 4 mM NADH, 2 mM ATP, creatine kinase 100 µg ml⁻¹, creatine phosphate 5 mM and succinate 2 mM) for 1h at 30 °C. 5 % of the reaction was set aside as input and the rest was diluted in SEM buffer (sucrose 2.5 M, 1 mM EDTA, 10 mM MOPS-KOH pH7.2) treated with proteinase K for 15 min on ice to assess mitochondrial import. After inhibition of proteinase K with 1 mM PMSF, mitochondria were centrifuged at 7000g for 10 min, washed once with SEM buffer and resuspended in 2x Laemmli buffer before separation by SDS-PAGE alongside the input samples and analysis on Phosphorimager.

2.10. Mass spectrometry (MS) analysis

For liquid chromatography-tandem mass spectrometry (LC-MS/MS) experiments of mitochondrial proteins associated with STAT3, samples both enriched and depleted with STAT3 were obtained using SDS and NP-40 extraction of mitochondrial lysates from mouse liver. Extracted samples were precipitated, resuspended in 6 M urea, 2 M Thiourea in 50 mM ammonium bicarbonate, pH 8.0 with Halt protease inhibitor cocktail (Thermo Fisher Scientific), reduced in 10 mM dithiothreitol (Sigma), and alkylated in 20 mM iodoacetamide (Sigma). Protein digestions were performed with mass spectrometry grade trypsin (16h, Promega, Inc.) at an enzyme to protein ratio of 1–50 (w/w). The tryptic peptides thus generated were purified using a C18 stage tip (3 M Empore, Bioanalytical Technologies) and analyzed by nanoLC-MS/MS on an Orbitrap Fusion Tribrid™ mass spectrometer (Thermo Fisher Scientific). A label-free quantification (LFQ) algorithm was applied to quantitatively determine the peptide enrichment in measured samples.

2.11. Analysis of MS data

For the data analysis of STAT3-associated mitochondrial proteome, the MaxQuant software (v.1.6.15.0) (<https://www.maxquant.org/>) with embedded Andromeda search engine was used. Mass spectra were searched against the UniProt-mouse database (<https://www.uniprot.org/proteomes/UP000000589>). Further data analysis was performed with the Perseus software (version 1.6.15.0) using the results files obtained from MaxQuant search. Proteins identified only by site, reverse database hits, and potential contaminants were removed, and replicate samples were grouped. Proteins with <2 out of 3 valid values in at least one group were removed, and missing values were imputed from a normal distribution around the detection limit. The final quantified protein list was used for downstream data analysis. Pathway analysis was performed by probing the Reactome 2022 pathway knowledgebase⁴⁵ by using the Enrichr tool,^{46,47} using as input all proteins enriched >1.5-fold in a particular fraction.

2.12. Complex I activity

Two micrograms of purified mitochondria were incubated in a 96-well plate with 100 μL of complex I assay buffer (25 mM KPO_4 , 2 mM KCN, 3.5 g L^{-1} BSA, 60 μM DCIP, 70 μM DCU, 1 μM antimycin A) with or without 10 μM rotenone for 10 min at 37 $^\circ\text{C}$. Five millimolar NADH was added to start the reaction, and absorbance was measured continuously at 600 nm at 30-s intervals for 10 min at 37 $^\circ\text{C}$. Complex I activity was defined as: 1 U = 1 μM DCIP reduced per min per μg of protein.

2.13. Mitochondrial membrane potential activity

Mitochondrial membrane potential was estimated from ψ_m measurements, as previously described.¹⁵ In brief, peripheral blood leukocytes were obtained from WT and STAT3-SA mice, stimulated *in vitro* with 40 ng/ml GM-CSF, and then incubated for 20 min in media containing 50 nM TMRE. TMRE fluorescence was detected in the far-red channel following excitation by a 488 nm laser and detection with an FL-2 bandpass filter by flow cytometry.

3. Results

3.1. STAT3 is partitioned between an NP-40 soluble and an SDS-soluble membrane compartment in the mitochondria

We and others have previously documented the presence of STAT3 in mitochondria, however, its exact sub-localization in the organelle remains somewhat ambiguous and is a subject of controversy. In order to better identify in what compartment STAT3 resides inside mitochondria, we subjected highly purified mitochondria isolated from mouse liver and heart to differential detergent purification. To this end, we performed sequential extractions using either the non-ionic detergent NP-40 or the ionic detergent SDS to obtain differentially soluble proteins. Protein extracts were subsequently analyzed by western blotting. The majority of mitochondrial STAT3 α was recovered in the SDS extracted fraction, although it was detectable in the NP-40 extract at lower abundance. As expected, the cytochrome C oxidase subunit COXVa, a membrane component of respiratory complex IV involved in oxidative phosphorylation, was entirely recovered in the NP40 extracted fraction (Fig. 1A). In contrast, significant portions of ATP5A and ATP5B, constituents of the membrane-spanning F_0 component of the ATP synthase complex V, were retained in the SDS fraction after NP-40 extraction (Fig. 1A and B). We obtained similar results with mitochondria purified from the osteosarcoma cell line 143b with STAT3 compartmentalizing partially in the NP-40 extracted fraction but mainly in the SDS fraction. Interestingly, phosphodiesterase (PDE), Cytochrome C1 (CytC1) and mitochondrial transcription factor A (TFAM) were also partitioned between both fractions (Fig. 1C). We confirmed these results using another cell line, namely the mammary adenocarcinoma MDA-MB-231. Again, we detected the presence of STAT3 mainly in the SDS extracts with a portion of the protein being recovered in the NP-40 extracted fraction. In this cell line, the mitochondrial proteins SDHA, ATP5b, NDUFS2 and Tom20 were mainly recovered after NP40 extraction, with only traces of these proteins being left in the SDS fraction after NP-40 extraction (Fig. 1D, left panel).

The fact that STAT3 was mainly recovered after SDS extraction, similar to TFAM, prompted us to examine the possibility that STAT3 interacted with the mitochondrial genome, thus

tethering it into a compartment only extractable with SDS. In order to test this hypothesis, we generated MDA-MB-231 cells devoid of mitochondrial DNA (MDA-MB-231 $\rho 0$) and monitored whether the absence of mitochondrial DNA would allow STAT3 to be released into the NP-40 fraction. As shown in the right panel of Fig. 1D, the presence of STAT3 in the SDS extracted fraction was not altered by depletion of mitochondrial DNA. Loss of mitochondrial DNA (mtDNA) in MDA-MB-231 $\rho 0$ cells was verified by quantitative PCR, demonstrating complete loss of detectable mtDNA in this cell line (Fig. 1E). In sum, mitochondrial STAT3 was found to reside mainly in an SDS-extractable compartment containing mtDNA-associated factors that were not solubilized by NP-40, but its retention in this compartment does not appear to require tethering to mitochondrial DNA.

3.2. The STAT3 mitochondrial fraction is enriched in respiratory complex proteins

To better understand STAT3 mitochondrial localization, we compared the protein content of the NP-40 and SDS soluble compartments. To this end, we purified mitochondria from mouse livers and sequentially extracted them with NP40 and SDS-containing buffers, as described. Triplicate samples from independent animals were then prepared for protein identification by mass spectrometry. Triplicate technical replicas of each individual triplicate biological sample were subjected to trypsin digestion, and the subsequent peptides were separated by LC-MS/MS.⁴⁸ Database searching with the resulting MS spectra was used to identify proteins within each fraction and each identified protein was quantified based on the abundance of constituent peptides. Label-free quantification identified 4013 unique proteins in the NP-40 fraction, including 2004 proteins identified and quantified in at least 2 out of 3 biological replicates. Similarly, 4013 unique proteins were identified in the SDS fraction, including 2529 proteins identified and quantified in at least 2 out of 3 biological replicates.

Comparison of the protein content of the NP-40 soluble and SDS soluble samples demonstrated that they were composed of largely distinct individual proteins (Fig. 2A). As expected, STAT3 itself was detected in the SDS-soluble sample, while it was undetectable in the NP-40 fraction, consistent with its reduced abundance in this fraction (see Fig. 1). To better understand the nature of the proteins that cofractionated with STAT3 during detergent extraction, we analyzed them by using the Reactome pathway knowledgebase,⁴⁵ identifying functional categories by using the Enrichr tool.^{46,47} Proteins that were >1.5-fold enriched in the NP40 soluble fraction relative to the SDS fraction were comprised largely of mitochondrial protein translation factors (Fig. 2B), such as translational elongation, initiation, and termination components and tRNA aminoacylation proteins. In contrast, proteins that were >1.5-fold enriched in the SDS fraction containing STAT3 compared to the NP40 fraction were composed largely of respiratory electron transport and citric acid cycle proteins (Fig. 2C). For instance, this fraction contained many of the subunit proteins of the complex I NADH dehydrogenase, such as Ndufs8, Ndufs4, Ndufa10, Ndufv3, Ndufs6, Ndufs7, Ndufb5, Ndufs3, Ndufa9, and Ndufs1. Several subunits of the complex IV cytochrome C oxidase were also present. The association of STAT3 with the respiratory electron transport chain is consistent with previous findings and with the mitochondrial phenotypes detected following STAT3 inhibition or loss.^{15,49} For instance, we previously showed that STAT3 associates with complex I proteins and that inhibition of STAT3 activity results in reduced complex I activity and impaired NAD⁺ regeneration.²⁰ Interestingly,

mitochondrial STAT3 has been recently reported to augment translational efficiency by participating in mRNA transport to active ribosomes,⁵⁰ consistent with the presence of translation factors along with low amounts STAT3 in the NP-40 extracts.

3.3. STAT3 exists in a multimeric form in the mitochondria and its N-terminal domain plays a role in its mitochondrial localization

Previous research has documented that STAT3 exists as a dimer, both in the cytoplasm and in the nucleus,⁵¹ mediated by homotypic interaction of the amino-terminal domain⁵² and phosphotyrosine-SH2 domain interactions.⁵ However, the potential dimeric state of STAT3 inside mitochondria in absence of tyrosine phosphorylation is still unclear. Unlike the similar protein STAT1, the core region of STAT3 does not dimerize in absence of tyrosine phosphorylation.⁵³ Therefore, to investigate the potential multimeric state of mitochondrial STAT3, we made use of a recombinant vector expressing Flag-tagged STAT3 fused to the biotin ligase domain (BioID2) driven to the mitochondria by adding a mitochondrial targeting sequence, encoding a chimeric STAT3 protein of 130 kDa (MTS.STAT3.Bio) that could be readily distinguished from endogenous STAT3 by size. After expression of this chimeric construct in MDA-MB-231 cells, we performed an immunoprecipitation using anti-Flag antibodies. Interestingly, immunoblotting with anti-STAT3 antibodies revealed that immunoprecipitation of the chimeric protein also pulled down endogenous STAT3, strongly suggesting that STAT3 dimerizes with itself in mitochondria (Fig. 3A). To rule out the possibility that the ~80 kDa STAT3 band was a degradation product of MTS.STAT3.Bio rather than endogenous STAT3, we expressed the construct in STAT3-null cells, which showed only the ~130 kDa MTS.STAT3.Bio construct (Supplemental Fig. 1). To further delineate the region of STAT3 implicated in this interaction, we then expressed a similar recombinant STAT3 protein except for a deletion of its C-terminal domain (MTS.TruncSTAT3.Bio). After performing an immunoprecipitation with anti-Flag antibodies followed by immunoblotting with anti-STAT3, we failed to detect endogenous STAT3 (Fig. 3B, upper panel). Of note, the epitope recognized by the anti-STAT3 antibody used is located in the C-terminus of STAT3, hence the product of MTS.TruncSTAT3.Bio cannot be detected. To ensure that the chimeric truncated STAT3 was indeed expressed, the immunoblot was reprobed with anti-Flag antibodies. As shown in the lower panel of Fig. 3B, MTS.TruncSTAT3.Bio is properly expressed and immunoprecipitated with anti-Flag antibodies. This result also confirms that the interactions detected between MTS.STAT3.Bio and endogenous STAT3 were mediated by STAT3 domains, not the tags added to artificial construct. Taken together, the results shown here demonstrate that in mitochondria, STAT3 interacts with itself via a motif present in the C-terminus of the protein to form a dimeric or possibly higher order complex.

We then sought to identify what domains of STAT3 were instrumental for its mitochondrial localization. In order to test the implication of the N-terminal domain of STAT3, we transfected HEK 293T cells engineered to lack endogenous STAT3 with a construct expressing either full length STAT3 (WT ST3) or a version of STAT3 lacking the first 132 amino acids (ΔNSTAT3).⁵⁴ Mitochondria from transfected cells were purified either by combined treatment with digitonin and trypsin to remove peripherally associated proteins⁴³ or by digitonin/trypsin treatment followed by sucrose gradient purification to remove

other intracellular organelles.⁴² Cytosolic and mitochondrial extracts were analyzed by immunoblot using anti-STAT3 antibodies. As expected, full length STAT3 α was readily detected in mitochondrial extracts regardless of the purification process used to produce the originating mitochondria preparations (Fig. 3D). In contrast, STAT3 missing its N-terminal domain was very poorly recovered in mitochondrial extracts (Fig. 3D), although it was readily detected in the cytosol. These data strongly suggest that a motif located in the first 132 amino acids of STAT3 is critical for mitochondrial localization. Antibodies against succinate dehydrogenase complex, subunit A (SDHA), UBQCR2 and tubulin were used to assess the absence of cross contamination between cytosolic and mitochondrial extracts (Fig. 3D, lower panels). Note that the SDHA blot was a reprobing of the previous STAT3 blot and that the bands detected in the cytosol in the SDHA blot represent residual reactivity from the previous detection of STAT3, distinct by size from SDHA.

3.4. STAT3 linker domain contains a mitochondrial targeting sequence

In order to take a more systematic approach to identification of the location of a mitochondrial targeting signal within STAT3, we decided to utilize an *in vitro* translocation system. This system analyzes translocation of *in vitro* translated ³⁵S-labeled protein across the membrane of isolated mitochondria. We first confirmed that *in vitro* translated STAT3 was indeed efficiently imported into mitochondria using this system (Fig. 4A, lanes 3 and 4), whereas Green Fluorescent Protein (GFP), used as a negative control, failed to accumulate in mitochondria (Fig. 4A, lanes 1 and 2). However, in contrast to GFP alone, when GFP is fused to a protein carrying a mitochondrial import signal, it can be efficiently imported inside mitochondria, as shown in Fig. 4A, lanes 5–8 using mitochondrial solute carrier (slc) as an example MTS. We decided to use this observation as a basis for searching for STAT3 import signals, and we fused different individual domains of STAT3 (F1–F6) to GFP to obtain proteins with an amenable size for this study. STAT3 fragments from F1 to F6, as shown in Fig. 4B, upper panel, were cloned under the control of the T7 promoter as fusions with GFP. Import into freshly purified mitochondria revealed that the fragment F4, corresponding to the linker domain of STAT3 that connects the DNA binding domain to the SH2 domain,⁵³ was the only fragment that efficiently translocated GFP into mitochondria (Fig. 4C, lanes 11 and 12). This result strongly suggested that a STAT3 internal mitochondrial targeting sequence was located inside the linker domain. It has been documented that, in general, mitochondrial targeting motifs are rich in positively charged amino acids with the potential to form amphipathic α -helices.⁵⁵ Analysis of the linker domain of STAT3 revealed 5 potential α -helices as shown in Fig. 4B, lower panel. We undertook to test the implication of each helix separately by mutating key positively charged amino acids (shown in red in Fig. 4B, lower panel). Each mutated F4 fragment termed M1 to M5 was then analyzed for its ability to translocate into mitochondria *in vitro*. All of the mutated F4 fragments showed equivalent capacity to be imported into mitochondria, suggesting a more complex mechanism possibly involving the cooperation of multiple motifs present in the linker domain (Fig. 4D). To further delineate the location of the mitochondrial targeting motif, we tested the amino-terminal portion (aa 495 to 535) and the carboxy-terminal portion (aa 536 to 583, corresponding to the final 2 α -helices) of the linker domain. When fused to GFP, only the carboxyl-terminal helices but not the amino-terminal helices mediated mitochondrial translocation (Fig. 4E).

3.5. C687/712 are not required for mitochondrial import but alter mitochondrial function

STAT3 was recently reported to be S-palmitoylated on two cysteine residues located in the C-terminal portion of the protein, C687 and C712,⁵⁶ although the functional significance of this post-translational modification remains unclear and some of the original data concerning this modification have been retracted.⁵⁷ In the original report, palmitoylation did not affect Y705 phosphorylation following cytokine stimulation; nonetheless, a STAT3 mutant lacking the implicated Cys residues showed decreased nuclear localization and reduced homodimerization.⁵⁶ Protein palmitoylation is known to regulate membrane localization and trafficking,⁵⁸ and cysteine residues have been implicated in mitochondrial protein import.⁵⁵ Therefore, we tested the potential role of residues C687 and C712 for the mitochondrial targeting of STAT3. To this end, we constructed expression plasmids carrying either a single mutation C687 into S, or a double mutation C687S/C712S (2CS). After expression in MDA-MB-231 cells deficient for endogenous STAT3, cytoplasmic and mitochondrial fractions were analyzed by immunoblot using anti-STAT3 antibodies. The ER protein calreticulin fractionated exclusively to the cytoplasmic sample and was excluded from the mitochondrial preparations containing STAT3, demonstrating the purity of these fractions. Partitioning of both singly or doubly mutated STAT3 between cytoplasm and mitochondria was not notably affected compared to the WT protein, strongly suggesting that neither cysteine residue 697 or 712 nor their post-translational modification is critical for STAT3 mitochondrial import (Fig. 5A). For completeness, we analyzed the residual pellet remaining after SDS lysis of mitochondria, which contained minimal amounts of STAT3 and other mitochondrial proteins.

Next, we explored whether the absence of C687 and C712 and their potential palmitoylation impacted STAT3 biological functions. We first tested the steady state level of expression of the typical STAT3 target gene, suppressor of cytokine signaling (SOCS) 3. As shown in Fig. 5B, loss of endogenous STAT3 in STAT3 KO cells led to a greater than 50 % decrease in expression of endogenous SOCS3. However, re-expression of WT or doubly mutant 2CS STAT3 in the KO cells restored expression of SOCS3 to WT levels. Therefore, we concluded that modification of C687 and C712 does not affect basal expression of STAT3 target genes. We then addressed mitochondrial functions of STAT3 by monitoring complex I activity in the same set of cells. As previously reported,²⁰ complex I activity was dramatically impaired in STAT3 deficient cells and this activity was fully restored by complementation with the WT form of STAT3. However, in cells expressing the mutant form of STAT3 lacking C687 and C712, complex I activity remained impaired (Fig. 5C). This result suggests that S-palmitoylation or some other function of these two cysteine residues is important for at least some STAT3 mitochondrial functions, although not for mitochondrial localization, potentially by affecting STAT3 interactions with other proteins or with membranes.

3.6. S727 phosphorylation is not essential for mitochondrial localization

The role of S727 phosphorylation in STAT3 mitochondrial function and localization has been a subject of controversy. While it is widely accepted that S727 is instrumental for a number of STAT3 mitochondrial functions, there is still a debate about its implication in the mitochondrial import of the protein.^{40,59,60} To examine the post-translational state of STAT3, we compared mitochondrial and cytoplasmic STAT3 by 2-dimensional gel

electrophoresis.⁶¹ Cytoplasmic and mitochondrial protein extracts from MDA-MB-231 cells were separated by isoelectric focusing followed by SDS-PAGE and the resulting gels were analyzed by immunoblotting for STAT3 (Fig. 6A). Both mitochondrial and cytoplasmic samples revealed major species with mobilities of approximately 88 kDa that resolved into several discrete isoelectric points. The mitochondrial sample also displayed species with a smaller apparent molecular weight of approximately 50 kDa, a possible proteolytic breakdown product. Importantly, the major mitochondrial STAT3 species displayed a notably more acidic isoelectric point relative to the major cytoplasmic STAT3 species, suggesting increased phosphorylation.

We next addressed the functional significance of STAT3 phosphorylation by altering the phosphorylation status of S727 by using Calyculin A (CalA), an inhibitor of the serine phosphatase PP2A that prevents the turnover of phospho-S727.⁶² Treatment of MDA-MB-231 cells with CalA increased the level of STAT3 S727 phosphorylation both in cytoplasmic and mitochondrial extracts. However, the overall level of mitochondrial STAT3 was unchanged after CalA treatment (Fig. 6B). CalA treatment did not affect the overall abundance of total STAT3 in either subcellular compartment or the abundance of the mitochondrial protein, NDUFB2. We concluded from these data that it was unlikely that phosphorylation of S727 was a critical driver of STAT3 mitochondrial import, since increased phosphorylation did not result in increased mitochondrial abundance.

To test the absolute requirement for S727 phosphorylation for mitochondrial import and function, we used our mouse model that expresses a knock-in (KI) mutant version of STAT3 (S727A) that cannot be phosphorylated. This model directly probes the necessity of pS727 in mitochondria. STAT3-S727A, referred to as SA, cannot be phosphorylated on S727 but is expressed from the STAT3 promoter at endogenous levels.^{63,64} Cytoplasm and mitochondria were purified from livers of WT and SA mice, and the cytoplasmic and mitochondrial protein extracts were assessed for the presence of STAT3 by immunoblotting. As shown in Fig. 6C, the mitochondrial abundance of STAT3 was comparable between WT STAT3 and STAT3 S727A. Purity of cytoplasmic and mitochondrial samples was confirmed by the partitioning of ERK1 in the cytoplasm and F1 ATPase in mitochondria. These results demonstrate that pS727 is not required for mitochondrial import since its absence does not affect the steady state abundance of STAT3 inside the mitochondria, even though S727 phosphorylation has been found to be critical for many STAT3 mitochondrial functions.^{15,16,22,23,60,65,66} To directly test the functional consequences of pS727, we compared the mitochondrial membrane potential of WT and SA cells. To this end, we isolated peripheral blood leukocytes from WT and SA mice, stimulated them *in vitro* with GM-CSF, and measured mitochondrial membrane potential by flow cytometry based on TMRE fluorescence.¹⁵ Consistent with results from STAT3-null cells, cells from SA mice demonstrated defective membrane potential (Supplementary Fig. 2), confirming that S727 phosphorylation is required for STAT3 mitochondrial function, even though it is not required for translocation.

4. Discussion

A large number of proteins have been mapped to mitochondria, the vast majority of which are encoded by the nuclear genome rather than the limited coding capacity of the mitochondrial genome.⁶⁷⁻⁶⁹ Interestingly, up to 50 % of mitochondrial proteins are also found in other subcellular locations outside of mitochondria,^{67,70} including nuclear transcription factors that also accumulate in mitochondria.⁷¹ For proteins mapped to multiple subcellular locations, their mitochondrial abundance can be either their major or their minor location. STAT3 falls into this latter category, with the majority of STAT3 partitioning between cytoplasm and nucleus with only a minor fraction localizing to mitochondria.^{15,16,18} The low abundance of mitochondrial STAT3 and a lack of understanding of its translocation mechanism have hindered a full appreciation of its physiological functions.

In this study, we showed that mitochondrial targeting of STAT3 involves protein motifs encoded within the amino-terminal domain and the linker domain. It has been previously reported that STAT3 acetylation provides a critical signal for mitochondrial translocation, at least in response to insulin stimulation, including acetylation of the amino-terminal domain.⁷² Involvement of amino-terminal acetylation in mitochondrial translocation of STAT3 is consistent with our finding that the amino-terminal domain is required for localization. The role of serine 727 phosphorylation in STAT3 localization has been more controversial, with some data suggesting it is required⁴⁰ while many published data do not show this requirement.^{59,72} Nonetheless, S727 phosphorylation contributes to the biochemical function of mitochondrial STAT3.⁷³ Since much of the experimental evidence for an involvement of pS727 in STAT3 mitochondrial translocation has been derived from manipulated cancer cells *in vitro*, we examined this issue in primary tissues of the mouse. Using a KI mouse model, we found equal mitochondrial accumulation of both WT and S727A mutant STAT3 in normal mouse liver, suggesting no absolute requirement for pS727 for localization.

Within mitochondria, STAT3 partitioned between two distinct compartments that could be distinguished on the basis of detergent solubility. A minor fraction of mitochondrial STAT3 was extracted by buffers containing the nonionic detergent NP-40, while the majority of mitochondrial STAT3 required the ionic detergent SDS for solubilization. The NP-40 soluble portion of STAT3 copurified mainly with mitochondrial translation factors while the SDS soluble portion copurified with components of the oxidative phosphorylation respiratory chain. While we cannot rule out the possibility that the small amount of STAT3 present in the NP-40 fractions is due at least in part to cytoplasmic contamination, the large enrichment of mitochondrial proteins in this fraction and the relative paucity of cytoplasmic proteins detected by mass spectrometry argues against this possibility. Interestingly, the Gough laboratory has recently reported that a portion of mitochondrial STAT3 binds the LRPPRC-SLIRP complex, regulating mitochondrial mRNA stability, ribosomal delivery, and protein translation kinetics.⁵⁰ It is conceivable that the NP-40 soluble STAT3 fraction participates in this process. Similarly, considerable research has shown functional and structural interactions between STAT3 and components of the oxidative phosphorylation chain, such as interactions with GRIM19^{39,40,74,75} and other components of respiratory

complex I.^{16,20,21} It is likely that the SDS soluble fraction of STAT3 identified in this study participates in the regulation of electron transport chain activity.

The mechanisms underlying the partitioning of STAT3 into differentially soluble compartments remain to be identified. However, we provide data on how STAT3 is initially targeted to mitochondria, despite it not containing an obvious mitochondrial targeting sequence. Our results show that at least two domains of STAT3 are involved in mitochondrial translocation. Removal of the amino-terminal 132 amino acids impaired STAT3 mitochondrial targeting, suggesting that this domain is required. Although amino-terminal targeting sequences represent a common mechanism of mitochondrial protein translocation, the STAT3 amino terminus does not appear to include a traditional presequence since it is not cleaved following translocation and it does not contain a series of basic residues. Moreover, although the amino terminal domain was necessary for STAT3 mitochondrial translocation, it was not itself sufficient to direct GFP into mitochondria, as would be expected for a typical mitochondrial targeting pre-sequence.⁵⁵ This domain of STAT3 contains an acetylation site that has been implicated in mitochondrial localization,⁷² which could explain at least in part its requirement for translocation. Of note, many proteins destined for the mitochondrial matrix and the inner membrane contain additional internal motifs that maintain them in an import-competent state and facilitate their correct targeting.^{76,77}

In contrast to the amino-terminal domain that was necessary for import but was insufficient to drive mitochondrial localization *in vitro* on its own, the linker domain of STAT3 contained a motif that was sufficient to direct GFP into mitochondria. This internal motif was localized to an alpha-helical domain at the carboxyl terminus of the linker domain, a region of STAT3 that has not as yet been assigned a precise function.⁷⁸ It has been shown that for many mitochondrial proteins lacking a classical pre-sequence, correct mitochondrial targeting is dependent on cooperation between multiple internal targeting motifs.⁷⁹ It is likely that mitochondrial STAT3 similarly depends on cooperation between amino-terminal and linker domain motifs. It will be of interest to determine if these motifs directly or indirectly interact with the mitochondrial transport machinery. Of note, GRIM-19, a protein that has been implicated in STAT3 mitochondrial translocation,⁴⁰ interacts with the STAT3 linker domain.³⁹ However, the requirement for phosphorylated S727 for the STAT3-GRIM-19 interaction⁷⁴ is in contrast to our finding that S727 is superfluous for mitochondrial translocation and that the carboxyl terminus of STAT3 containing S727 is incapable of directing import. Therefore, it is likely that additional roles for the linker domain in this process beyond GRIM-19 interaction still need to be discovered.

STAT3 exists in both monomeric and dimeric conformations,⁸⁰ until dimerization is stabilized by phosphotyrosine-SH2 domain interactions,⁵³ unlike STAT1 which appears to form spontaneous stable dimers whether or not it is phosphorylated.^{81,82} We found that mitochondrial STAT3, which is not phosphorylated on tyrosine 705, nonetheless is capable of forming homodimers or multimers. There are multiple dimerization interfaces within the STAT3 structure, including within the coiled-coil and SH2 domains.⁸³ We found that mitochondrial STAT3 multimerization depended on the carboxyl-terminal region of the protein, including the SH2 and transactivation domains, since deletion of this region

abrogated interaction with endogenous STAT3. It is possible that the SH2 domain mediates STAT3 dimerization in mitochondria, even in the absence of phosphotyrosine. Further studies will be required to fully elucidate the stoichiometry of these complexes.

Palmitoylation of the STAT3 SH2/transactivation domain has been suggested to promote dimerization.⁵⁶ We found that the cysteine residues that are the major sites for palmitoylation were not required for translocation of STAT3 to mitochondria. However, mutation of these residues abrogated a major function of mitochondrial STAT3, namely its ability to augment respiratory complex I activity. In contrast, mutation of these residues did not affect the canonical nuclear function of STAT3 as a transcription factor. It is possible that palmitoylation of STAT3 affects its dimerization or another critical interaction that is required to augment complex I enzymatic activity, such as interaction with partner proteins or with membranes.

5. Conclusions

In sum, the current study resolves a number of previously unanswered or controversial issues concerning the mechanisms and function of mitochondrial STAT3. Although the presence of STAT3 in mitochondria has been challenged,^{13,17} there is considerable evidence in the literature for both the physical presence and the functional consequences of mitochondrial STAT3. Here, we show that STAT3 fractionates with highly purified mitochondria prepared by a variety of methods, including those that result in mitochondria that are devoid of proteins associated with the endoplasmic reticulum and mitochondrial-associated membranes. It has also been reported that STAT3 is associated with mitochondrial DNA, at least in some cell types.⁸⁴ However, we show here that the presence of STAT3 in mitochondria is not affected by depletion of the mitochondrial genome and therefore does not require interaction with DNA for mitochondrial localization. Similarly, it has been suggested that mitochondrial translocation of STAT3 is dependent on phosphorylation of S727.^{40,59} However, we find that the abundance of STAT3 in mitochondria isolated from mouse tissues is unaffected by mutation of S727 and therefore does not require its phosphorylation for localization. The role of STAT3 palmitoylation has also been questioned.⁵⁷ Although we did not directly address palmitoylation, we show that the cysteine residues that are potential sites for lipid modification are required for the full mitochondrial activity of STAT3, but not for its translocation. Future studies will be required to identify the biological function of these cysteine residues. Finally, we identify the regions of STAT3 that comprise the signals involved in mitochondrial targeting by showing that loss of the amino-terminal domain abrogates mitochondrial translocation and that a carboxyl-terminal helix from the linker domain contains a mitochondrial targeting motif. It will be of interest in the future to determine how these sequence motifs target STAT3 translocation and whether these or additional motifs are required to partition STAT3 between distinct locations within mitochondria that are defined by differential detergent solubility and which we speculate are involved in the distinct mitochondrial functions of enhancing the efficiency of translation⁵⁰ and of augmenting respiratory complex I activity.^{15,16,20}

Supplementary Material

Refer to Web version on PubMed Central for supplementary material.

Acknowledgments

We thank Maher Abdul-Hay for measuring the membrane potential of STAT3-SA cells, Yeray Arteaga and Liang Hu for expert technical assistance, and Lara Brambilla for advice and discussions. This work was funded in part by the National Institutes of Health grant AI28900 and by a grant from the Feinberg Lymphoma Foundation.

Abbreviations

CalA	Calyculin A
CytC1	Cytochrome C1
ER	Endoplasmic reticulum
GFP	Green Fluorescent Protein
GRIM	Gene associated with retinoid-interferon induced mortality
JAK	Janus kinase
KI	Knock-in
MAM	Mitochondria-associated membranes
Slc	Mitochondrial solute carrier
SOCS	Suppressor of cytokine signaling
STAT	Signal transducer and activator of transcription
TFAM	Mitochondrial transcription factor A
TIM	Translocase of the inner membrane
TOM	Translocase of the outer membrane

References

1. Akira S, Nishio Y, Inoue M, et al. Molecular cloning of APRF, a novel IFN-stimulated gene factor 3 p91-related transcription factor involved in the gp130-mediated signaling pathway. *Cell*. 1994;77:63–71. [PubMed: 7512451]
2. Zhong Z, Wen Z, Darnell JE. Stat3: a STAT family member activated by tyrosine phosphorylation in response to epidermal growth factor and interleukin-6. *Science*. 1994;264:95–98. [PubMed: 8140422]
3. Raz R, Durbin JE, Levy DE. Acute phase response factor and additional members of the interferon-stimulated gene factor 3 family integrate diverse signals from cytokines, interferons, and growth factors. *J Biol Chem*. 1994;269:24391–24395. [PubMed: 7523373]
4. Schaefer TS, Sanders LK, Park OK, Nathans D. Functional differences between Stat3alpha and Stat3beta. *Mol Cell Biol*. 1997;17:5307–5316. [PubMed: 9271408]
5. Levy DE, Darnell JE Jr. STATs: transcriptional control and biological impact. *Nat Rev Mol Cell Biol*. 2002;3(9):651–662. [PubMed: 12209125]

6. Ng IH, Ng DC, Jans DA, Bogoyevitch MA. Selective STAT3- α or- β expression reveals spliceform-specific phosphorylation kinetics, nuclear retention and distinct gene expression outcomes. *Biochem J.* 2012;447(1):125–136. [PubMed: 22799634]
7. Decker T, Lew DJ, Cheng YS, Levy DE, Darnell JE. Interactions of alpha- and gamma-interferon in the transcriptional regulation of the gene encoding a guanylate-binding protein. *EMBO J.* 2009;8:2009–2014, 1989.
8. Levy DE, Lee CK. What does Stat3 do? *J Clin Invest.* 2002;109:1143–1148. [PubMed: 11994402]
9. Yang J, Chatterjee-Kishore M, Staugaitis SM, et al. Novel roles of unphosphorylated STAT3 in oncogenesis and transcriptional regulation. *Cancer Res.* 2005;65:939–947. [PubMed: 15705894]
10. Yang J, Stark GR. Roles of unphosphorylated STATs in signaling. *Cell Res.* 2008;18 (4):443–451. [PubMed: 18364677]
11. Liu B, Palmfeldt J, Lin L, et al. STAT3 associates with vacuolar H(+)-ATPase and regulates cytosolic and lysosomal pH. *Cell Res.* 2018;28(10):996–1012. [PubMed: 30127373]
12. Avalle L, Camporeale A, Morciano G, et al. STAT3 localizes to the ER, acting as a gatekeeper for ER-mitochondrion Ca(2+) fluxes and apoptotic responses. *Cell Death Differ.* 2019;26(5):932–942. [PubMed: 30042492]
13. Su Y, Huang X, Huang Z, Huang T, Xu Y, Yi C. STAT3 localizes in mitochondria-associated ER membranes instead of in mitochondria. *Front Cell Dev Biol.* 2020;8:274. [PubMed: 32391361]
14. Vassilev AO, Lorenz DR, Tibbles HE, Uckun FM. Role of the leukemia-associated transcription factor STAT3 in platelet physiology. *Leuk Lymphoma.* 2002;43(7):1461–1467. [PubMed: 12389630]
15. Gough DJ, Corlett A, Schlessinger K, Wegrzyn J, Larner AC, Levy DE. Mitochondrial STAT3 supports Ras-dependent oncogenic transformation. *Science.* 2009;324(5935):1713–1716. [PubMed: 19556508]
16. Wegrzyn J, Potla R, Chwae YJ, et al. Function of mitochondrial Stat3 in cellular respiration. *Science.* 2009;323(5915):793–797. [PubMed: 19131594]
17. Harhous Z, Badawi S, Bona NG, et al. Critical appraisal of STAT3 pattern in adult cardiomyocytes. *J Mol Cell Cardiol.* 2019;131:91–100. [PubMed: 31022374]
18. Phillips D, Reilley MJ, Aponte AM, et al. Stoichiometry of STAT3 and mitochondrial proteins: implications for the regulation of oxidative phosphorylation by protein-protein interactions. *J Biol Chem.* 2010;285(31):23532–23536. [PubMed: 20558729]
19. Meier JA, Hyun M, Cantwell M, et al. Stress-induced dynamic regulation of mitochondrial STAT3 and its association with cyclophilin D reduce mitochondrial ROS production. *Sci Signal.* 2017;10(472).
20. Lahiri T, Brambilla L, Andrade J, Askenazi M, Ueberheide B, Levy DE. Mitochondrial STAT3 regulates antioxidant gene expression through complex I-derived NAD in triple negative breast cancer. *Mol Oncol.* 2021;15(5):1432–1449. [PubMed: 33605027]
21. Brambilla L, Lahiri T, Cammer M, Levy DE. STAT3 inhibitor OPB-51602 is cytotoxic to tumor cells through inhibition of complex I and ROS induction. *iScience.* 2020;23(12), 101822. [PubMed: 33305182]
22. Gough DJ, Marie IJ, Lobry C, Aifantis I, Levy DE. STAT3 supports experimental K-RasG12D-induced murine myeloproliferative neoplasms dependent on serine phosphorylation. *Blood.* 2014;124(14):2252–2261. [PubMed: 25150294]
23. Poli V, Camporeale A. STAT3-Mediated metabolic reprogramming in cellular transformation and implications for drug resistance. *Front Oncol.* 2015;5:121. [PubMed: 26106584]
24. Kleinbongard P. Perspective: mitochondrial STAT3 in cardioprotection. *Basic Res Cardiol.* 2023;118(1):32. [PubMed: 37620559]
25. Szczepanek K, Chen Q, Larner AC, Lesnfsky EJ. Cytoprotection by the modulation of mitochondrial electron transport chain: the emerging role of mitochondrial STAT3. *Mitochondrion.* 2012;12(2):180–189. [PubMed: 21930250]
26. Rincon M, Pereira FV. A new perspective: mitochondrial Stat3 as a regulator for lymphocyte function. *Int J Mol Sci.* 2018;19(6):1656. [PubMed: 29866996]

27. Valenca-Pereira F, Fang Q, Marie JJ, et al. IL-6 enhances CD4 cell motility by sustaining mitochondrial Ca(2+) through the noncanonical STAT3 pathway. *Proc Natl Acad Sci U S A*. 2021;118(37).
28. Yu H, Lee H, Herrmann A, Buettner R, Jove R. Revisiting STAT3 signalling in cancer: new and unexpected biological functions. *Nat Rev Cancer*. 2014;14(11):736–746. [PubMed: 25342631]
29. Wang HQ, Man QW, Huo FY, et al. STAT3 pathway in cancers: past, present, and future. *MedComm*. 2020;3(2):e124, 2022.
30. Ahting U, Thieffry M, Engelhardt H, Hegerl R, Neupert W, Nussberger S. Tom40, the pore-forming component of the protein-conducting TOM channel in the outer membrane of mitochondria. *J Cell Biol*. 2001;153(6):1151–1160. [PubMed: 11402060]
31. Wang Q, Guan Z, Qi L, et al. Structural insight into the SAM-mediated assembly of the mitochondrial TOM core complex. *Science*. 2021;373(6561):1377–1381. [PubMed: 34446444]
32. Araiso Y, Tsutsumi A, Qiu J, et al. Structure of the mitochondrial import gate reveals distinct preprotein paths. *Nature*. 2019;575(7782):395–401. [PubMed: 31600774]
33. Eilers M, Schatz G. Binding of a specific ligand inhibits import of a purified precursor protein into mitochondria. *Nature*. 1986;322(6076):228–232. [PubMed: 3016548]
34. Matouschek A, Azem A, Ratliff K, Glick BS, Schmid K, Schatz G. Active unfolding of precursor proteins during mitochondrial protein import. *EMBO J*. 1997;16(22):6727–6736. [PubMed: 9362487]
35. Neupert W, Brunner M. The protein import motor of mitochondria. *Nat Rev Mol Cell Biol*. 2002;3(8):555–565. [PubMed: 12154367]
36. Rassow J, Hartl F-U, Guiard B, Pfanner N, Neupert W. Polypeptides traverse the mitochondrial envelope in an extended state. *FEBS Lett*. 1990;275(1-2):190–194. [PubMed: 2148157]
37. Neupert W, Herrmann JM. Translocation of proteins into mitochondria. *Annu Rev Biochem*. 2007;76:723–749. [PubMed: 17263664]
38. Vogtle FN, Wortelkamp S, Zahedi RP, et al. Global analysis of the mitochondrial N-proteome identifies a processing peptidase critical for protein stability. *Cell*. 2009;139(2):428–439. [PubMed: 19837041]
39. Lufei C, Ma J, Huang G, et al. GRIM-19, a death-regulatory gene product, suppresses Stat3 activity via functional interaction. *EMBO J*. 2003;22:1325–1335. [PubMed: 12628925]
40. Tammineni P, Anugula C, Mohammed F, Anjaneyulu M, Larner AC, Sepuri NB. The import of the transcription factor STAT3 into mitochondria depends on GRIM-19, a component of the electron transport chain. *J Biol Chem*. 2013;288(7):4723–4732. [PubMed: 23271731]
41. Khozhukhar N, Spadafora D, Rodriguez Y, Alexeyev M. Elimination of mitochondrial DNA from mammalian cells. *Curr Protoc Cell Biol*. 2018;78(1), 20 11 21–20 11 14.
42. Clayton DA, Shadel GS. Purification of mitochondria by sucrose step density gradient centrifugation. *Cold Spring Harb Protoc*. 2014;2014(10). doi:10.1101/008028. [PubMed: 25275106]
43. Dixit B, Vanhoozer S, Anti NA, O'Connor MS, Boominathan A. Rapid enrichment of mitochondria from mammalian cell cultures using digitonin. *MethodsX*. 2021;8, 101197. [PubMed: 34434723]
44. Kim DI, Roux KJ. Filling the void: proximity-based labeling of proteins in living cells. *Trends Cell Biol*. 2016;26(11):804–817. [PubMed: 27667171]
45. Jassal B, Matthews L, Viteri G, et al. The reactome pathway knowledgebase. *Nucleic Acids Res*. 2020;48(D1):D498–D503. [PubMed: 31691815]
46. Chen EY, Tan CM, Kou Y, et al. Enrichr: interactive and collaborative HTML5 gene list enrichment analysis tool. *BMC Bioinf*. 2013;14:128.
47. Kuleshov MV, Jones MR, Rouillard AD, et al. Enrichr: a comprehensive gene set enrichment analysis web server 2016 update. *Nucleic Acids Res*. 2016;44(W1):W90–W97. [PubMed: 27141961]
48. Lim MS, Elenitoba-Johnson KSJ. Proteomics in pathology research. *Lab Invest*. 2004;84(10):1227–1244. [PubMed: 15311217]
49. Joanna Wegrzyn RP, Chwae Yong-Joon, Naresh B, et al. Function of mitochondrial Stat3 in cellular respiration. *Science*. 2009;323.

50. Fernando CD, Jayasekara WSN, Inampudi C, et al. A STAT3 protein complex required for mitochondrial mRNA stability and cancer. *Cell Rep.* 2023;42(9), 113033. [PubMed: 37703176]
51. Braunstein J, Brutsaert S, Olson R, Schindler C. STATs dimerize in the absence of phosphorylation. *J Biol Chem.* 2003;278(36):34133–34140. [PubMed: 12832402]
52. Ota N, Brett TJ, Murphy TL, Fremont DH, Murphy KM. N-domain-dependent nonphosphorylated STAT4 dimers required for cytokine-driven activation. *Nat Immunol.* 2004;5:208–215. [PubMed: 14704793]
53. Ren Z, Mao X, Mertens C, et al. Crystal structure of unphosphorylated STAT3 core fragment. *Biochem Biophys Res Commun.* 2008;374(1):1–5. [PubMed: 18433722]
54. Zhang L, Badgwell DB, Bevers JJ 3rd, et al. IL-6 signaling via the STAT3/SOCS3 pathway: functional analysis of the conserved STAT3 N-domain. *Mol Cell Biochem.* 2006;288:179–189. [PubMed: 16718380]
55. Wiedemann N, Pfanner N. Mitochondrial machineries for protein import and assembly. *Annu Rev Biochem.* 2017;86(1):685–714. [PubMed: 28301740]
56. Niu J, Sun Y, Chen B, et al. Fatty acids and cancer-amplified ZDHHC19 promote STAT3 activation through S-palmitoylation. *Nature.* 2019;573(7772):139–143 [Retracted]. [PubMed: 31462771]
57. Niu J, Sun Y, Chen B, et al. Retraction Note: fatty acids and cancer-amplified ZDHHC19 promote STAT3 activation through S-palmitoylation. *Nature.* 2020;583 (7814), 154–154. [PubMed: 32555452]
58. Wang Y, Lu H, Fang C, Xu J. Palmitoylation as a signal for delivery. *Adv Exp Med Biol.* 2020;1248:399–424. [PubMed: 32185719]
59. Peron M, Dinarello A, Meneghetti G, et al. Y705 and S727 are required for the mitochondrial import and transcriptional activities of STAT3, and for regulation of stem cell proliferation. *Development.* 2021;148(17).
60. Gough DJ, Koetz L, Levy DE. The MEK-ERK pathway is necessary for serine phosphorylation of mitochondrial STAT3 and Ras-mediated transformation. *PLoS One.* 2013;8(11), e83395. [PubMed: 24312439]
61. O'Farrell PH. High resolution two-dimensional electrophoresis of proteins. *J Biol Chem.* 1975;250(10):4007–4021. [PubMed: 236308]
62. Woetmann A, Nielsen M, Christensen ST, et al. Inhibition of protein phosphatase 2A induces serine/threonine phosphorylation, subcellular redistribution, and functional inhibition of STAT3. *Proc Natl Acad Sci U S A.* 1999;96(19):10620–10625. [PubMed: 10485875]
63. Shen Y, La Perle KM, Levy DE, Darnell JE Jr. Reduced STAT3 activity in mice mimics clinical disease syndromes. *Biochem Biophys Res Commun.* 2005;330:305–309. [PubMed: 15781265]
64. Shen Y, Schlessinger K, Zhu X, et al. Essential role of STAT3 in postnatal survival and growth revealed by mice lacking STAT3 serine 727 phosphorylation. *Mol Cell Biol.* 2004;24:407–419. [PubMed: 14673173]
65. Gough DJ, Sehgal PB, Levy DE. Nongenomic functions of STAT3. In: Decker T, Müller M, eds. *Jok-Stat Signaling: From Basics to Disease.* Wien: Springer-Verlag GmbH; 2012:91–98.
66. Garama DJ, White CL, Balic JJ, Gough DJ. Mitochondrial STAT3: powering up a potent factor. *Cytokine.* 2016;87:20–25. [PubMed: 27269970]
67. Thul P, Åkesson L, Wiking M, et al. A subcellular map of the human proteome. *Science.* 2017;356, eaal3321. [PubMed: 28495876]
68. Floyd BJ, Wilkerson EM, Veling MT, et al. Mitochondrial protein interaction mapping identifies regulators of respiratory chain function. *Mol Cell.* 2016;63(4):621–632. [PubMed: 27499296]
69. Calvo SE, Clauser KR, Mootha VK. MitoCarta2. 0: an updated inventory of mammalian mitochondrial proteins. *Nucleic Acids Res.* 2016;44(D1):D1251–D1257. [PubMed: 26450961]
70. Chong YT, Koh JL, Friesen H, et al. Yeast proteome dynamics from single cell imaging and automated analysis. *Cell.* 2015;161(6):1413–1424. [PubMed: 26046442]
71. Szczepanek K, Lesnefsky EJ, Larner AC. Multi-tasking: nuclear transcription factors with novel roles in the mitochondria. *Trends Cell Biol.* 2012;22(8):429–437. [PubMed: 22705015]
72. Xu YS, Liang JJ, Wang Y, et al. STAT3 undergoes acetylation-dependent mitochondrial translocation to regulate pyruvate metabolism. *Sci Rep.* 2016;6(1), 39517. [PubMed: 28004755]

73. Toši I, Frank DA. STAT3 as a mediator of oncogenic cellular metabolism: pathogenic and therapeutic implications. *Neoplasia*. 2021;23(12):1167–1178. [PubMed: 34731785]
74. Zhang J, Yang J, Roy SK, et al. The cell death regulator GRIM-19 is an inhibitor of signal transducer and activator of transcription 3. *Proc Natl Acad Sci U S A*. 2003;100:9342–9347. [PubMed: 12867595]
75. Huang G, Lu H, Hao A, et al. GRIM-19, a cell death regulatory protein, is essential for assembly and function of mitochondrial complex I. *Mol Cell Biol*. 2004;24:8447–8456. [PubMed: 15367666]
76. Backes S, Hess S, Boos F, et al. Tom70 enhances mitochondrial preprotein import efficiency by binding to internal targeting sequences. *JCB (J Cell Biol)*. 2018;217(4):1369–1382. [PubMed: 29382700]
77. Boos F, Mühlhaus T, Herrmann JM. Detection of internal matrix targeting signal-like sequences (iMTS-Ls) in mitochondrial precursor proteins using the TargetP prediction tool. *Bio-protocol*. 2018;8(17):e2474. [PubMed: 34395785]
78. Mertens C, Haripal B, Klinge S, Darnell JE. Mutations in the linker domain affect phospho-STAT3 function and suggest targets for interrupting STAT3 activity. *Proc Natl Acad Sci U S A*. 2015;112(48):14811–14816. [PubMed: 26553978]
79. Hansen KG, Herrmann JM. Transport of proteins into mitochondria. *Protein J*. 2019;38(3):330–342. [PubMed: 30868341]
80. Novak U, Ji H, Kanagasundaram V, Simpson R, Paradiso L. STAT3 forms stable homodimers in the presence of divalent cations prior to activation. *Biochem Biophys Res Commun*. 1998;247(3):558–563. [PubMed: 9647732]
81. Mao X, Ren Z, Parker GN, et al. Structural bases of unphosphorylated STAT1 association and receptor binding. *Mol Cell*. 2005;17(6):761–771. [PubMed: 15780933]
82. Zhong M, Henriksen MA, Takeuchi K, et al. Implications of an antiparallel dimeric structure of nonphosphorylated STAT1 for the activation-inactivation cycle. *Proceedings of the National Academy of Sciences of the USA*. 2005;102(11):3966–3971. [PubMed: 15753310]
83. Menon PR, Doudin A, Gregus A, Wirths O, Staab J, Meyer T. The anti-parallel dimer binding interface in STAT3 transcription factor is required for the inactivation of cytokine-mediated signal transduction. *Biochim Biophys Acta Mol Cell Res*. 2021;1868(12), 119118. [PubMed: 34390807]
84. Carbognin E, Betto RM, Soriano ME, Smith AG, Martello G. Stat3 promotes mitochondrial transcription and oxidative respiration during maintenance and induction of naive pluripotency. *EMBO J*. 2016;35(6):618–634. [PubMed: 26903601]

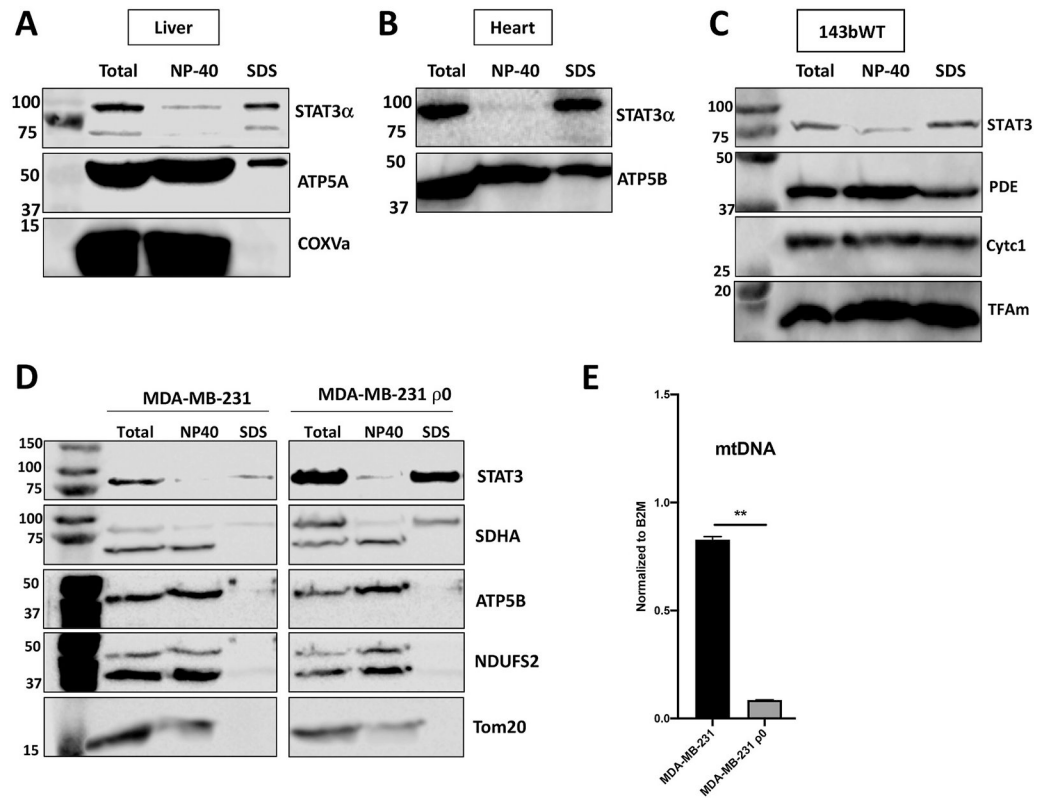


Fig. 1. Mitochondrial STAT3 partitions between an NP40-soluble and an SDS-soluble compartment.

Purified mitochondria from mouse liver (A), heart (B) or 143b cells (C) were sequentially extracted in the presence of NP-40 (NP-40) or SDS (SDS) as indicated. Protein extracts were separated on SDS-PAGE and analyzed by immunoblotting using the indicated antibodies. (D) Mitochondrial extracts from MDA-MB-231 cells (left panel) or MDA-MB-231 cells lacking mitochondrial DNA (MDA-MB-231 rho0 (ρ0)) (right panel) were performed as in A-C before being resolved on SDS-PAGE and probed with the indicated antibodies. (E) Quantification of mitochondrial DNA (mtDNA) in MDA-MB-231 rho0 (ρ0) and parental MDA-MB-231 cells by qPCR, p-value <0.05.

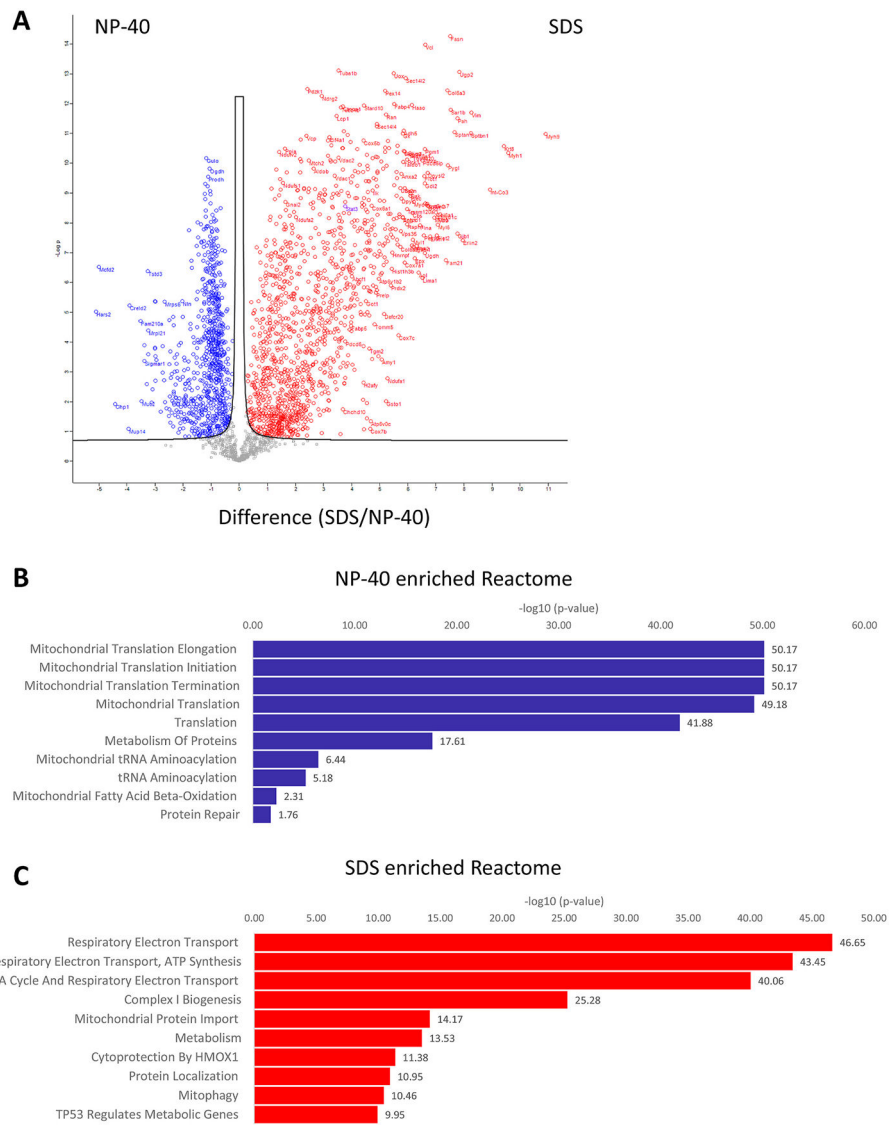


Fig. 2. Mass spectrometry analysis of NP-40 and SDS mitochondrial fractions. Volcano plot of protein abundance found respectively in NP-40 extracted fraction (NP-40) and SDS-extracted fraction (SDS). Arrow indicates STAT3. Reactome 2022 pathway analysis of proteins enriched in the NP-40 fractions (B) or SDS fractions (C).

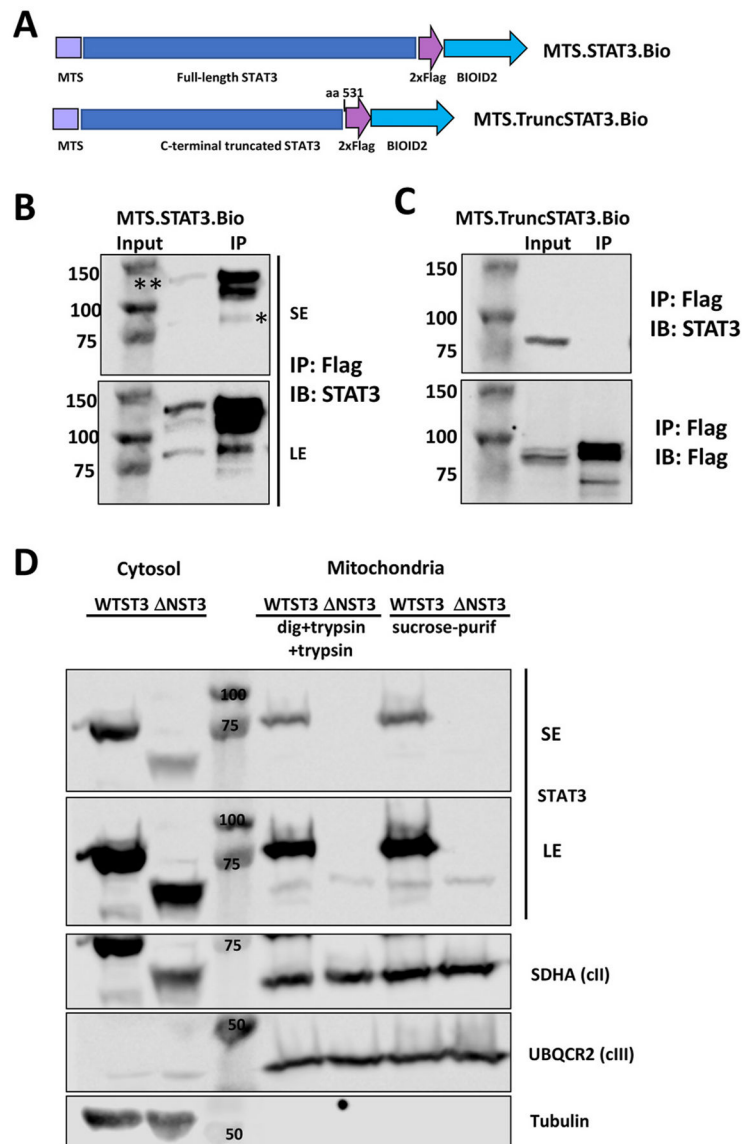


Fig. 3. STAT3 exists in a multimeric form in the mitochondria and its N-terminal domain plays a role in its mitochondrial localization.

(A) Graphic representation of recombinant STAT3 constructs. Mitochondrial extracts from MDA-MB-231 cells expressing MTS.STAT3.Bio (B) or MTS.TruncSTAT3.Bio (C) were immunoprecipitated with anti-Flag antibodies and immunoblotted with either STAT3 or Flag antibodies as indicated. Asterisk (*) marks endogenous STAT3. (D) Cytosolic (Cytosol) or mitochondrial (Mitochondria) extracts generated by 2 distinct purification protocols from HEK293T cells expressing either full length STAT3 (WTSTAT3) or STAT3 missing the first 132 amino acids (NST3) were analyzed by SDS-PAGE followed by immunoblotting using antibodies against STAT3, SDHA, UBQCR2 and Tubulin. SE: short exposure. LE: long exposure.

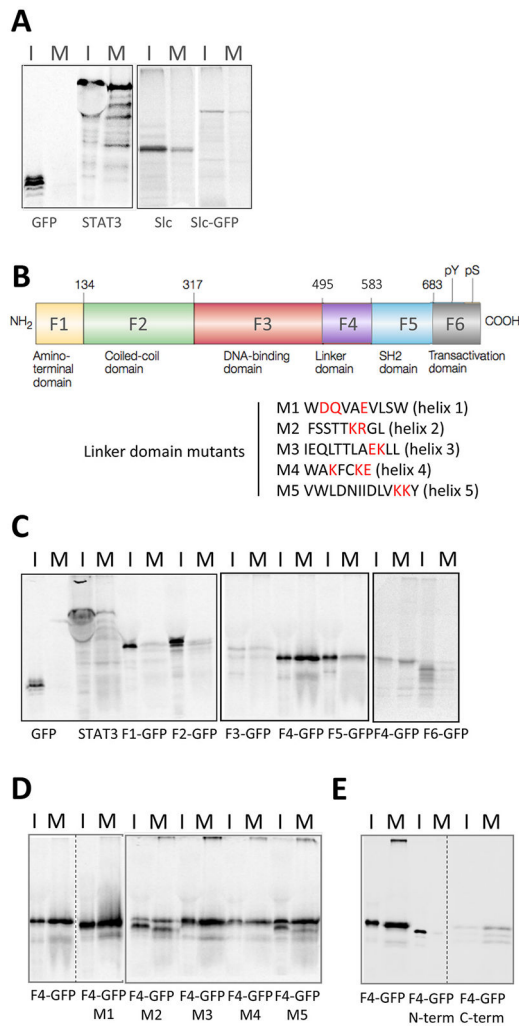


Fig. 4. A region of the linker domain of STAT3 contains a functional mitochondrial targeting motif.

In vitro translated ³⁵S-labeled GFP, STAT3, Slc and Slc-GFP were incubated with freshly prepared mitochondria. Input fractions (I) were resolved on SDS-page alongside the mitochondria imported fraction (M) to probe mitochondrial import efficiency. (B) Graphic map of the different functional domains of STAT3 (upper panel). Description of STAT3 linker domain mutants M1 to M5. Residues highlighted in red were mutated to alanine (lower panel). (C) *In vitro* mitochondrial import of STAT3 domains F1 to F6 fused to GFP (as described in A). (D) *In vitro* mitochondrial import of mutant M1 to M5 (as described in B) of linker domain F4 fused to GFP (as described in A). Lanes 1–2 showing fragment F4 (delineated by a dotted line) is the same image as lanes 11–12 of panel C, reshown to allow direct comparison. (E) As in (D), *in vitro* mitochondrial export of F4-GFP compared to its N-terminal fragment (F4-GFP N-term) and C-terminal fragment (F4-GFP C-term).

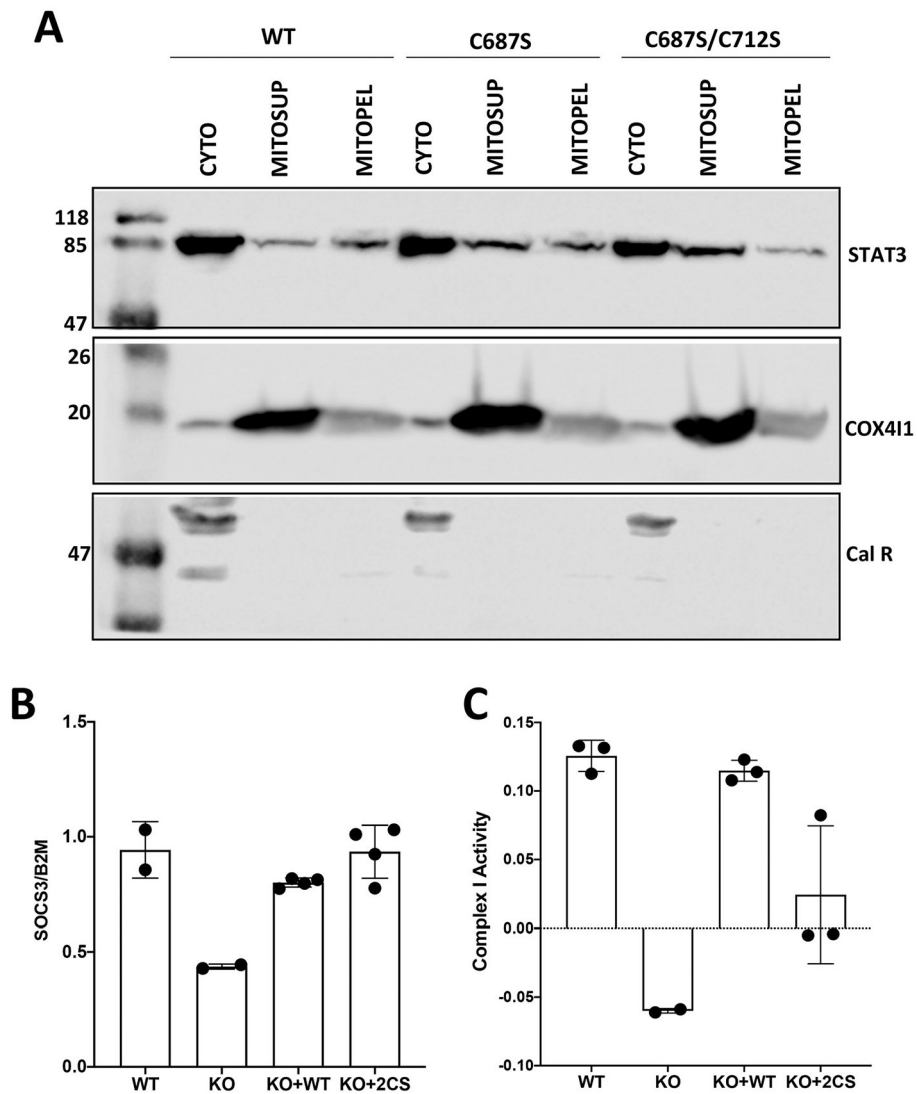


Fig. 5. C687/712 are not essential for mitochondrial import of STAT3.

(A) Cytoplasmic (CYTO) and mitochondrial extracts (MITO) as well as remaining residual pellet (PEL) of MDA-MB-231 cells deficient for endogenous STAT3 but ectopically expressing WT STAT3 (WT) or STAT3 mutated on C687 (C687S) or STAT3 doubly mutated on C687 and C712 (C687/C712S) were analyzed by SDS-PAGE and western blotting and probed with antibodies against STAT3, Cox411 and calreticulin (CalR). (B) Quantification of the STAT3 target gene SOCS3 mRNA levels by RT-qPCR normalized to B2M mRNA levels in STAT3 WT cells (WT), STAT3 KO cells (KO), STAT3 KO cells ectopically expressing either WT STAT3 (KO + WT) or STAT3 carrying the double mutation C6787S/C712S (KO+2CS). (C) Complex I activity of the set of cell lines described in B.

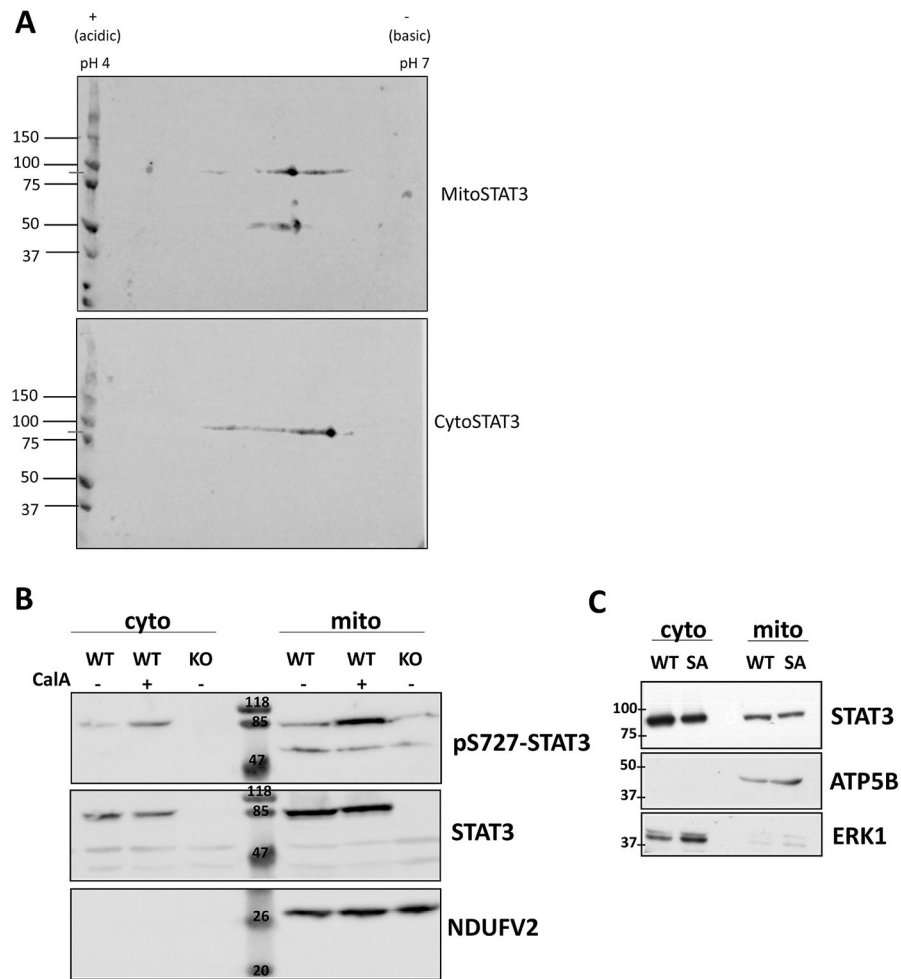


Fig. 6. S727 is not essential for mitochondrial localization.

(A) Cytoplasmic (CytoSTAT3) and mitochondrial (MitoSTAT3) protein extracts from MDA-MB-231 cells were separated by isoelectric focusing followed by SDS-PAGE and then analyzed by immunoblotting for STAT3. (B) MDA-MB-231 cells either carrying WT STAT3 (WT) or deleted for STAT3 (KO) were treated with Calyculin A (CalA) or left untreated. Cytoplasmic (cyto) and mitochondrial (mito) extracts were separated on SDS-PAGE and probed for pS727-STAT3, total STAT3 (STAT3) or NDUFV2 by western blot. (C) Cytoplasmic and mitochondrial extracts from livers of WT mice (WT) and mice homozygous for a knock-in mutant of STAT3 where serine727 is replaced by alanine (SA) were analyzed by SDS-PAGE and immunoblotting using antibodies against STAT3, F1 ATPase and ERK1.